Collinear splitting effects in direct detection of cosmic ray boosted dark matter

Jinmian Li

四川大學 SICHUAN UNIVERSITY

Aug. 22nd, 2025

Dark Matter and Neutrino Focus Week
TDLI, SJTU

Based on JHEP 02 (2023) 068; work in progress

with Zirong Chen, Shao-Feng Ge, Junle Pei, Feng Yang, Cong Zhang

Outline

1. The collinear splitting for boosted particle
   - Cosmic ray boosted self-interacting DM
2. Dark matter final state radiation (FSR) during acceleration
3. Dark matter parton distribution function (PDF) during recoiling

Photon radiation from charged particle

The probability of an electron to emit a collinear photon with a fraction x of its energy, is given by the Weizsaicker-Williams effective photon approximation

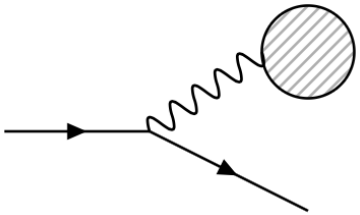

$$f_\gamma(x) \sim \frac{\alpha}{2\pi} P_{\gamma\ell}(x) \ln \frac{E^2}{m_\ell^2}$$

- The spliting function $P_{\gamma/\ell}(x) = (1 + (1-x)^2)/x$.
- The photon virtuality is $-p_T^2/(1-x)$, to the first order approximation.
- The photon propagator $\frac{1}{(p_a - p_b)^2} \sim \frac{1}{2E_a E_b(1-\cos\theta)}$

The parton distribution function

At the high energy scattering ($E \gg m$), process of collinear emission of initial state can be factorized into PDFs, given the collinear factorization formula. At muon collider,

$$\sigma_{\mu^+\mu^-\to X}(s) = \sum_{ij} \int dz_1\, dz_2 f_{i/\mu^+}(z_1) f_{j/\mu^-}(z_2) \hat{\sigma}_{ij\to X}(z_1 z_2 s)$$

The large logarithms in the splitting can be resumed with the DGLAP equation:

$$\frac{df_i(x, Q^2)}{d\log Q^2} = \sum_I \frac{\alpha_I}{2\pi} \sum_j P^I_{i,j}(x) \otimes f_j(x, Q^2)$$

- The factorization scale Q
- The index I loops over all possible interactions of particle i
- The initial condition at $Q^2 = m_\mu^2$ is $f_\mu(x, m_\mu^2) = \delta(1-x)$, and other PDFs vanish

Jet formation: the parton shower

The copious collinear radiations produce a collimated spray of particles, dubled jet.

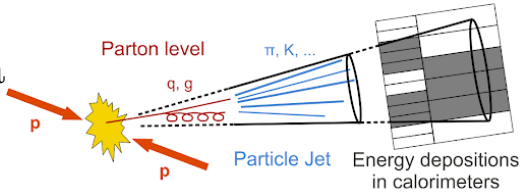

For a collinear emission:

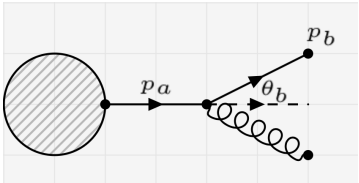

$$\sigma_{n+1} \sim \sigma_n \int \frac{dp_a^2}{p_a^2} \int dz \frac{\alpha_s}{2\pi} \hat{P}(z) \equiv \sigma_n \int dt W(t)$$

splitting kernel $\hat{P}(z)$, $z = E_b/E_a$, virtuality $t = p_a^2$

With multiple emissions

$$\sigma_{n+m} \sim \sigma_n \cdot \int dt_1 \cdots \int dt_m W(t_1) \cdots W(t_m)$$

$$\equiv \sigma_n \cdot \frac{1}{m!} (\int dt W(t))^m$$

In the collinear limit the cross section factorizes. The splitting can be iterated.

Jet formation: the parton shower

The probability for the next emission at t:

$$d\text{Prob}(t) = dtW(t)\exp(-\int_{t_0}^{t} dtW(t))$$

$\exp(-\int dtW(t))$ is Sudakov form factor = No emission probability

Monte Carlo description for the parton shower process

- Evolve the virtuality from $t^{\max}$ to $t^{\min}$, calculate the Sudakov form factor for each step
- Use veto algorithm to find the next splitting scale t, determine the splitting process
- Construct the splitting kinematics (off-shell mass, angular ordering)

Dark matter observations

- Dark matter existence seems evident

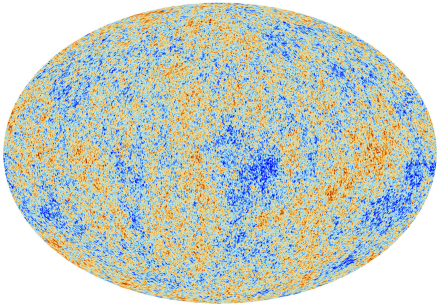

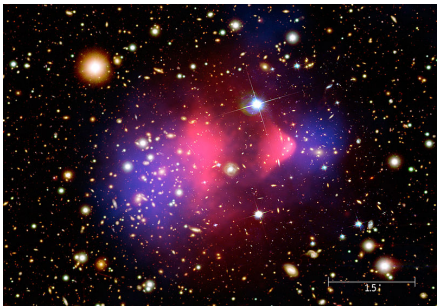

- Small scale structure problems

Core-vs-cusp (dwarfs, LSBs)

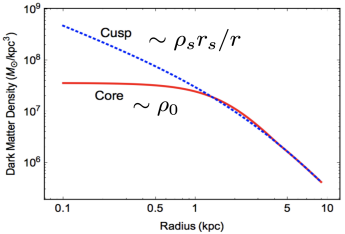

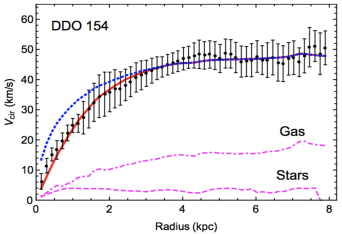

Central densities of halos are too shallow.

Too-Big-to-Fail (MW dwarf galaxies)

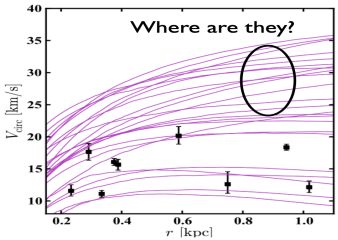

- Biggest predicted subhalos from CDM simulations
- Brightest observed galaxies in the MW

Predicted Milky Way satellites more massive (larger velocity dispersions) than observed ones.

Interactions in the dark matter sector

$\sigma/m \sim [1, 10]$ cm^2/g

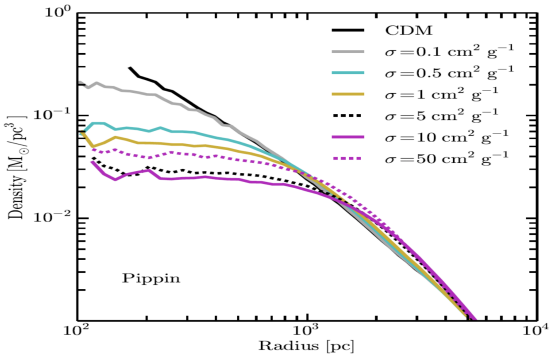

$\sigma/m \lesssim 1$ cm^2/g

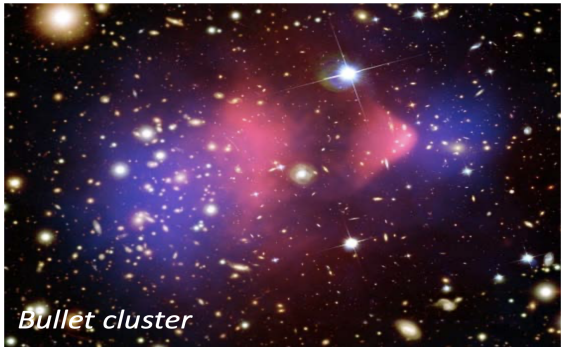

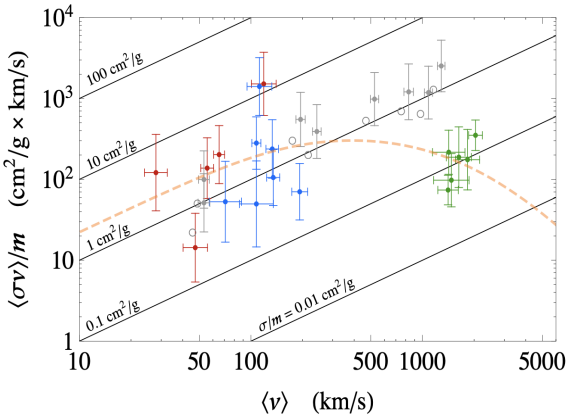

. *Kaplinghat, Tulin, Yu (PRL 2015)*

Favors a mild v-dependence

- Dwarfs
- LSBs
- Galaxy clusters

Boosted dark matter with new interactions?

Boosted DM in direct detection

The halo DM in space can be kicked by cosmic rays to have relativistic speed, and probed by detector on ground

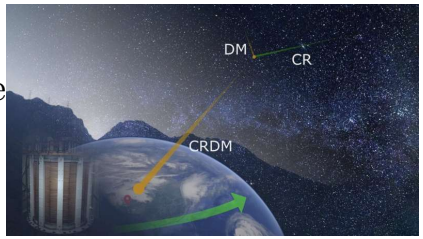

Electron-philic interaction:

$$\mathcal{L} \supset \epsilon \times g_{\rm em} A'_\mu \bar{e}\gamma^\mu e + g' A'_\mu \bar{\chi}\gamma^\mu \chi$$

The recoil flux of CR-induced DM (CRDM):

$$\frac{d\Phi_\chi}{dT_\chi} = D_{\rm eff} \frac{\rho_\chi^{\rm local}}{m_\chi} \int_{T_{\rm CR}^{\rm min}}^{\infty} dT_{\rm CR} \frac{d\Phi_e}{dT_{\rm CR}} \frac{d\sigma_{\chi e}}{dT_\chi}$$

DM scattered by energetic cosmic ray (CR):

$$\frac{d\sigma_{\chi e}}{dT_\chi} = g'^2 (\epsilon g_{\rm em})^2 \frac{2m_\chi (m_e + T_{\rm CR})^2 - T_\chi \left((m_e + m_\chi)^2 + 2m_\chi T_{\rm CR}\right) + m_\chi T_\chi^2}{4\pi (2m_e T_{\rm CR} + T_{\rm CR}^2)(2m_\chi T_\chi + m_A^2)^2}$$

CR boosted dark matter flux

Taking $g' = 1$, $\epsilon = 1$, $m_{A'} = 1$ MeV

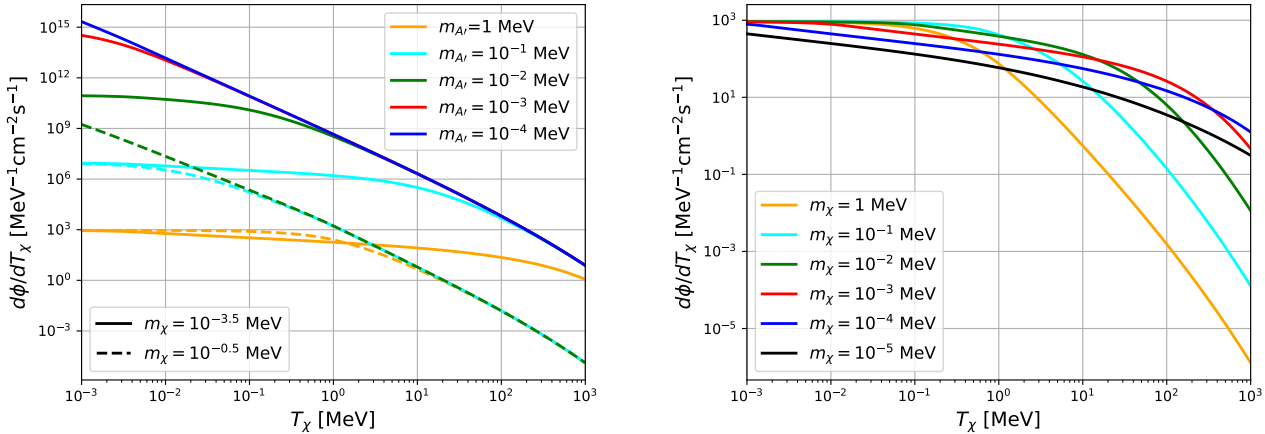

- For light DM and low T_χ, the flux is proportional to $m_{A'}^{-4}$
- For light DP, flux of heavy DM is much lower than light DM
- The differential flux is more flat for lighter DM and heavier dark photon, *i.e.*, higher fraction of high energy DM

The splitting functions for the dark sector

Interaction between Dirac fermion DM χ ($\bar{\chi}$) and dark photon A':

$$\mathcal{L} \supset g' A'_\mu \bar{\chi} \gamma^\mu \chi$$

Splitting function:

$$\frac{d\mathcal{P}_{A\to B+C}}{dz dk_T^2} \simeq \frac{1}{N} \frac{1}{16\pi^2} \frac{z\bar{z}\left|M_{\text{split}}\right|^2}{\left(k_T^2 + \bar{z} m_B^2 + z m_C^2 - z\bar{z} m_A^2\right)^2}$$

$A \to B + C$	$\frac{d\mathcal{P}_{A\to B+C}}{dz dk_T^2} = P_{A\to B+C}(z)$
$\chi/\bar{\chi} \to A'_T + \chi/\bar{\chi}$	$\frac{\alpha'}{2\pi} k_T^2 \frac{\frac{1+\bar{z}^2}{z} - \frac{\bar{z}}{z}\frac{2m_\chi^2 z^2 + m_{A'}^2\left(1+\bar{z}^2\right)}{k_T^2 + m_\chi^2 z^2 + m_{A'}^2 \bar{z}}}{k_T^2 + m_\chi^2 z^2 + m_{A'}^2 \bar{z}}$
$\chi/\bar{\chi} \to A'_L + \chi/\bar{\chi}$	$\frac{\alpha'}{\pi} k_T^2 \frac{m_{A'}^2 \bar{z}^2}{z\left(k_T^2 + m_\chi^2 z^2 + m_{A'}^2 \bar{z}\right)^2}$
$A'_T \to \bar{\chi}/\chi + \chi/\bar{\chi}$	$\frac{\alpha'}{2\pi} k_T^2 \frac{z^2 + \bar{z}^2 + \frac{z\bar{z}\left(2m_\chi^2 + m_{A'}^2\left(z^2+\bar{z}^2\right)\right)}{k_T^2 + m_\chi^2 - m_{A'}^2 z\bar{z}}}{k_T^2 + m_\chi^2 - m_{A'}^2 z\bar{z}}$
$A'_L \to \bar{\chi}/\chi + \chi/\bar{\chi}$	$\frac{2\alpha'}{\pi} k_T^2 \frac{m_{A'}^2 z^2 \bar{z}^2}{\left(k_T^2 + m_\chi^2 - m_{A'}^2 z\bar{z}\right)^2}$

Table 1: Splitting functions involving χ, $\bar{\chi}$, and A'.

The final state radiation

Sudakov Form Factor:

$$\Delta_A(Q_2;Q_1)\equiv\exp\left[-\sum_{BC}\int_{\ln Q_1^2}^{\ln Q_2^2} d\ln Q^2\int_{z_{\min}(Q)}^{z_{\max}(Q)} dz\ \frac{d\mathcal{P}_{A\to B+C}(z,Q)}{dz\ d\ln Q^2}\right]$$

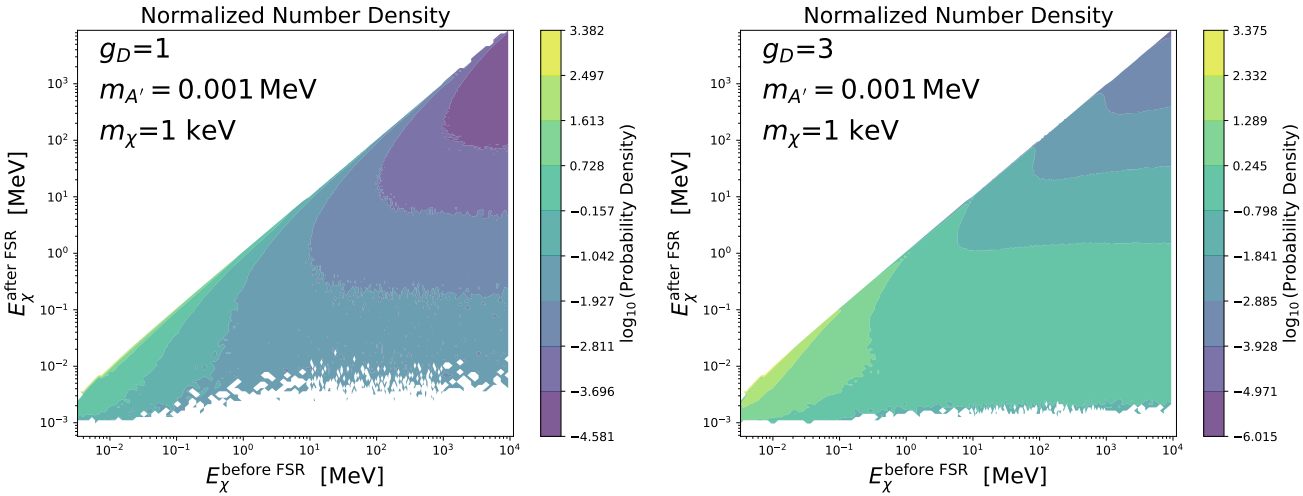

- Evolution range: $Q_{\max}\equiv\sqrt{t}=\sqrt{2m_\chi T_\chi},\ Q_{\min}=m_\chi+m_{A'}$
- Kinetic limit: $z_{\min}(Q)\equiv\frac{Q^2+m_B^2-m_C^2-\sqrt{(Q^2-m_B^2-m_C^2)^2-4m_B^2m_C^2}}{2Q^2}$,

  $z_{\max}(Q)\equiv\frac{Q^2+m_B^2-m_C^2+\sqrt{(Q^2-m_B^2-m_C^2)^2-4m_B^2m_C^2}}{2Q^2}$

CRDM flux with FSR

The evolution kernel $\mathcal{F}(E_\chi^{\text{before FSR}}, E_\chi^{\text{after FSR}})$

$$\frac{d\Phi_\chi}{dT_\chi} = \int \frac{d\Phi_\chi^0}{dT_\chi^0} \mathcal{F}\left(T_\chi^0 + m_\chi, T_\chi + m_\chi\right) dT_\chi^0$$

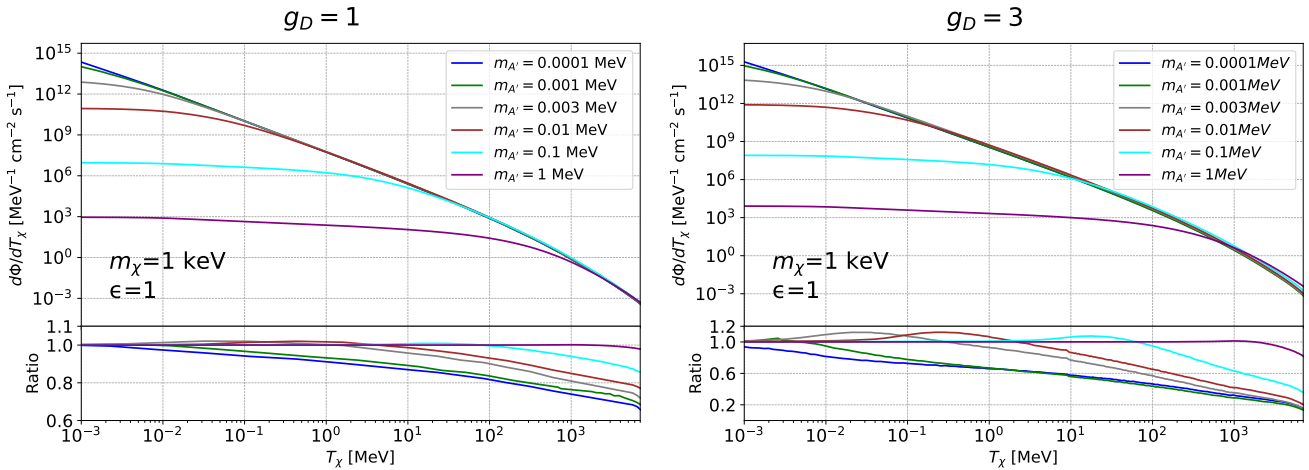

- FSR depletes the high-energy CRDM through the FSR.
- Enhances low-energy CRDM through radiated dark photon decay. The steeply falling DM flux renders the enhancement mild.

Signal rate at DM direct detection experiments

A boosted CRDM scattering off an electron in target atom:

$$\chi\left(p_1\right)+e^{-}\left(p_2\right)\rightarrow\chi\left(k_1\right)+e^{-}\left(k_2\right)$$

Initial bounded electrons effective mass $m_{\text{eff}}^2=(m_e-E_B^{nl})^2-\mathbf{p}^2$

The differential cross section with respect to the electron recoil kinetic energy T_R:

$$\begin{aligned}d\sigma_{nl}=&\sum_{nlms}\frac{1}{2E_\chi 2\left(m_e-E_B^{nl}\right)}\frac{d^3k_2}{(2\pi)^3 2E_{k_2}}\frac{d^3k_1}{(2\pi)^3 2E_{k_1}}\frac{d^3p_2}{(2\pi)^3}(2\pi)^4\delta^4\left(p_1+p_2-k_1-k_2\right)\\&\times\left|iM\left(\mathbf{p_1},\mathbf{p_2},\mathbf{k_1},\mathbf{k_2}\right)\right|^2\left|\psi_{nlm}\left(\mathbf{p_2}\right)\right|^2\\=&\frac{2l+1}{16\cdot(2\pi)^5}\frac{T_R\left|\mathbf{p_2}\right|}{E_\chi\left(m_e-E_B^{nl}\right)\left|\mathbf{p_1}\right|}\left|iM\left(p_1,p_2,k_1,k_2\right)\right|^2\left|\chi_{nl}\left(\left|\mathbf{p_2}\right|\right)\right|^2 d\phi_{p_2}\,d\left|\mathbf{p_2}\right|\,dq d\ln T_R\end{aligned}$$

The ionization rate:

$$\frac{dR_{ion}}{d\ln T_R}=\sum_{nl}N_T\int dT_\chi\frac{d\sigma_{nl}}{d\ln T_R}\frac{d\phi_\chi}{dT_\chi}$$

DM scattering at neutrino detectors - higher threshold

Boosted CRDM scattering off free electron ($T_\chi \gg E_B^{nl}$):

$$\chi(p_1) + e^-(p_2) \to \chi(k_1) + e^-(k_2)$$

The differential cross section of the electron recoil kinetic energy T_R:

$$\frac{d\sigma}{d\ln T_R} = \frac{1}{32\pi} \frac{T_R}{|\mathbf{p_1}|\, E_\chi m_e} |iM_{\chi e}|^2$$

The ionization rate (without distinguishing different shells) :

$$\frac{dR_{ion}}{d\ln T_R} = N_e \int dT_\chi \frac{d\sigma}{d\ln T_R} \frac{d\Phi_\chi}{dT_\chi}$$

The recoiling spectra ($g_D = 3$)

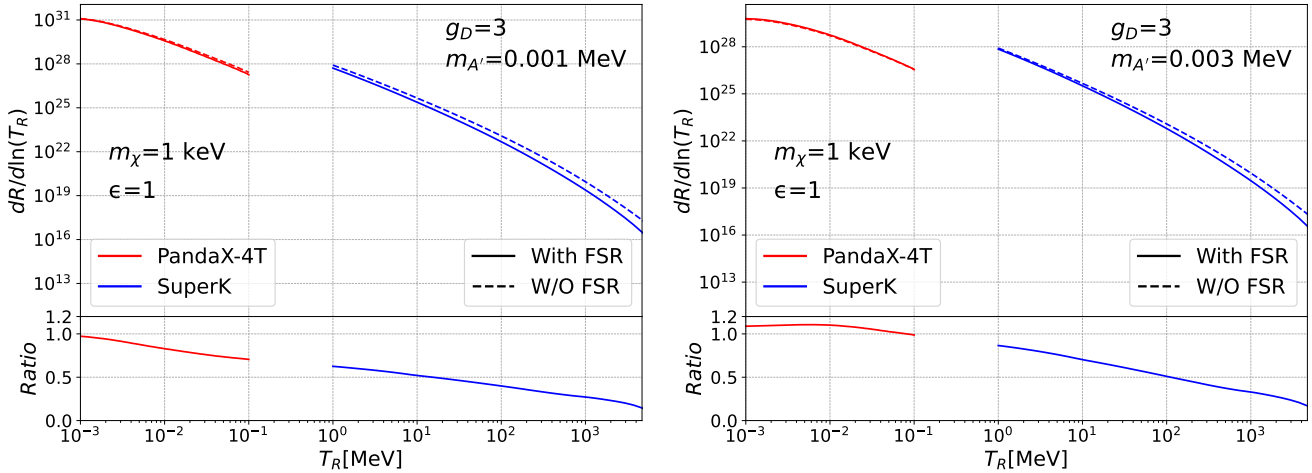

- PandaX-4T: 1.0 tonne-year exposure
- Super-K experiment: data taking period of 2628.1 days
- Enhancement at low T_R when $A' \to \chi\chi$ is allowed

Bounds from PandaX, Super-K, JUNO

- PandaX-4T::

$$\chi^2 = \sum_{i}^{\text{Run0,Run1}} \left(\frac{R^i_\chi + R^i_{\text{B}_0} - R^i_{\text{exp}}}{\sigma_i} \right)^2$$

90% C.L. limit obtained by $\Delta\chi^2 = \chi^2 - \chi^2_{\text{B}_0} = 2.71$

- Super-K: 161.9 kiloton-year exposure data, the total measured number of events N_{sk} is 4042 in the bin $0.1 < T_e/\text{GeV} < 1.33$. We require the DM signal $\xi \times N_{\text{DM}} < N_{\text{sk}}$, with signal efficiency $\xi = 0.93$.
- JUNO: one-year exposure with its 20-kiloton liquid scintillator target ($N_e = 6.744 \times 10^{33}$). Constraint obtained by requiring 10 events per year with $T_R > 10$ MeV.

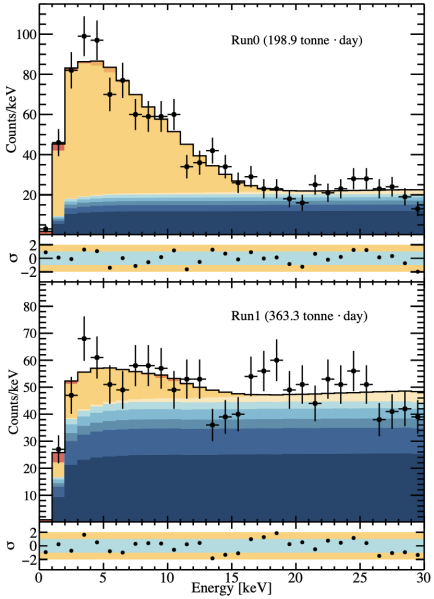

	100 MeV< E_{vis} < 1.33 GeV		
	Data	ν-MC	ϵ_{sig}(0.5 GeV)
FCFV	15206	14858.1	97.7%
& single ring	11367	10997.4	95.8%
& e-like	5655	5571.5	94.7%
& 0 decay-e	5049	5013.8	94.7%
& 0 neutrons	4042	3992.9	93.0%

FSR effects on the bounds

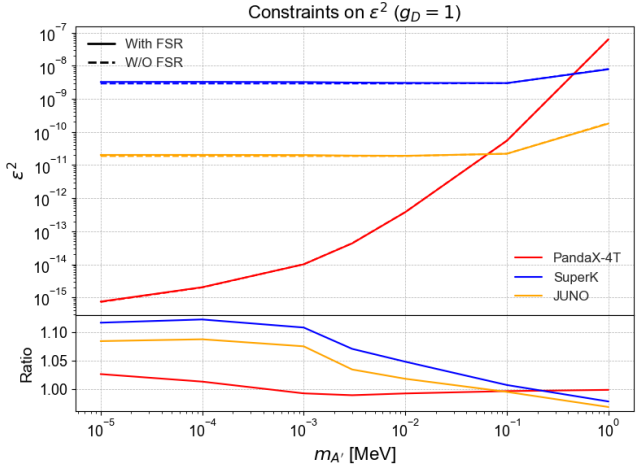

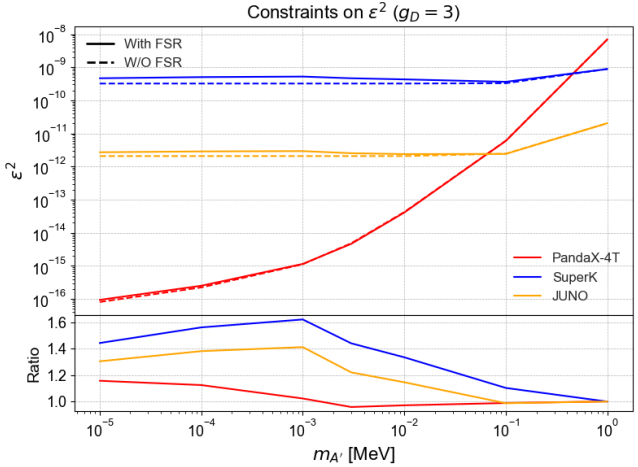

- Super-K and JUNO, which have higher energy thresholds, exhibit better sensitivity than PandaX-4T in the heavier m'_A regime.
- The FSR effects tend to relax the bounds by reducing the recoil rates
- Slightly strength the bound of PandaX-4T experiment especially for $m'_A \sim 3 \times 10^{-3}$ MeV

The DGLAP equations and DM PDF

DGLAP equations of PDFs:

$$\frac{df_i\left(k_T, x\right)}{d\ln k_T^2} = \sum_{m,n} N \int_x^1 \frac{dz}{z} P_{m\to i+n}(z) f_m\left(k_T, \frac{x}{z}\right) - \sum_{j,k} \int_0^1 dz P_{i\to j+k}(z) f_i\left(k_T, x\right)$$

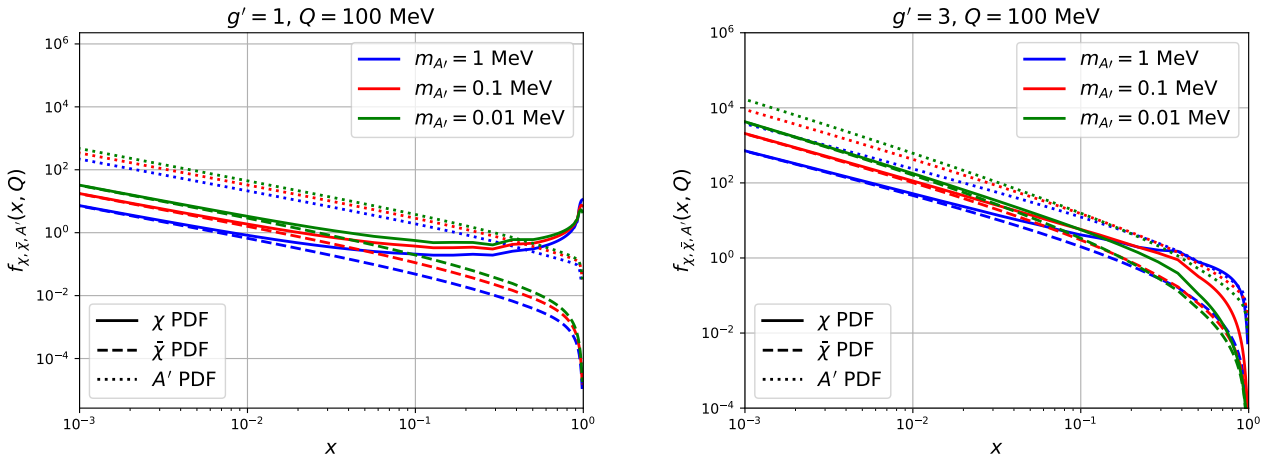

- There is large fraction of A' in the DM PDF, for large g', small x and lighter A' ($m_\chi = 0.01$ MeV).
- Approaching the perturbative limit $g' = 3$, f_χ no longer has the peak around $x \sim 1$

CRDM signal at the neutrino detectors: higher energy threshold

- Considering the DM PDFs becomes necessary as we primarily focus on a parameter region where the masses of DM and dark photon are significantly smaller than the typical energy scale of DM-electron scattering in neutrino detectors.
- The ionization rate:

$$\frac{dR_{ion}}{d\ln T_R} = N_T^{SK}\sum_i \int dT_\chi^0 \int_0^{x_{\max}} dx \frac{d\sigma^i}{d\ln T_R} f_i(Q,x) \frac{d\phi_\chi}{dT_\chi^0}\Theta(xE_\chi^0 - E_i^{\min}) + N_T^{SK}\int dT_\chi \frac{d\sigma_\chi}{d\ln T_R}\frac{d\phi_\chi}{dT_\chi}\Theta(T_\chi - T_\chi^{\min})\int_{x_{\max}}^1 f_\chi(Q,x)$$

- The index i in the PDF runs over χ, $\bar{\chi}$, and A', corresponding to the scattering processes $\chi + e^- \to \chi + e^-$, $\bar{\chi} + e^- \to \bar{\chi} + e^-$, and $A' + e^- \to \gamma + e^-$, respectively.

The PDF effects on Super-K bounds

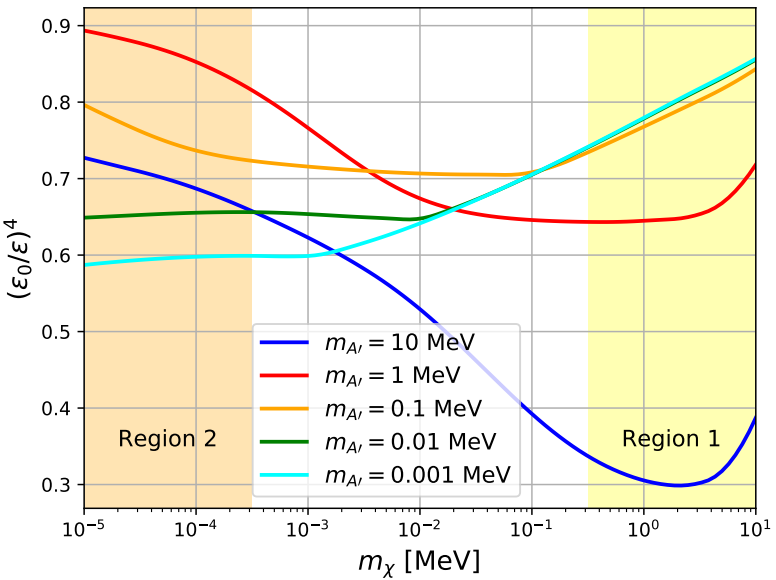

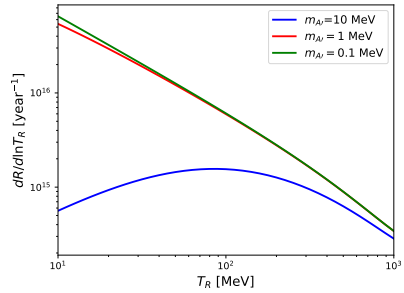

fix T_χ

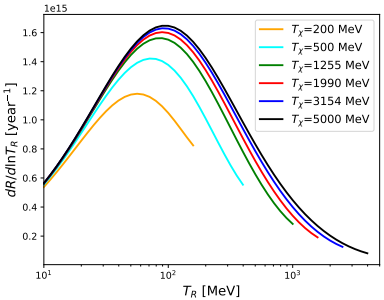

fix $m_{\chi,A'}$

- The DM PDF effects always reduce the experimental sensitivity ($g' = 1$)
- In region 1, typical energy scale of DM-electron scattering for heavier dark photon case is higher, leading to more significant PDF effects
- In region 2, the PDF effects are most significant when the signal DM flux is dominated by the DM with kinetic energy $T_\chi \sim \mathcal{O}(100)$ MeV

The dark photon signal: dark Compton scattering

Dark Compton scattering:

$$A' + e^- \to \gamma + e^-$$

The corresponding recoil rate:

$$\frac{dR}{d\ln E_\gamma} = N_T^{SK} \int dT_\chi^0 \int_0^{x_{\max}} dx \frac{d\sigma^{A'}}{d\ln E_\gamma} f_{A'}(Q,x) \frac{d\phi_\chi}{dT_\chi^0} \times \Theta(xE_\chi^0 - E_{A'\gamma}^{\min})\Theta(E_{A'\gamma}^{\max} - xE_\chi^0)$$

The Super-K is a water-based Cherenkov detector in which the Cherenkov rings produced by photons and electrons exhibit similarities. It is challenging to distinguish a mono-energetic photon with a threshold of $\mathcal{O}(1) \sim \mathcal{O}(10)$ MeV.

The PDF effects: photon signal at SuperK

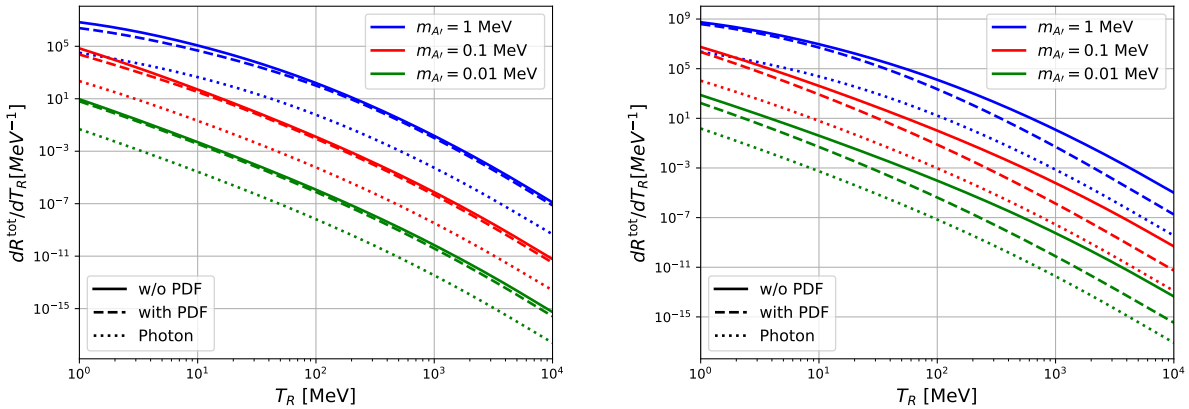

Figure 6: The differential recoil rate (at Super-K with data taking of 2628.1 days) for recoiled electron without DM PDF effects (solid line), with DM PDF effects (dashed line) and for the outgoing photon (dotted line), where we have taken fixed dark photon mass as indicated in the legend, DM mass $m_\chi = 0.01$ MeV, signal efficiency $\xi = 0.93$ and the ϵ is chosen as the maximal value that satisfies the XENON1T and Super-K bounds. Left panel: DM coupling $g' = 1$; Right panel: DM coupling $g' = 3$. [arXiv: 2209.10816]

Detecting the dark photon at DUNE and JUNO

- The DUNE and JUNO detectors possess high-efficiency photon identification capabilities.
- In these detectors, an energetic single photon signal can be considered background-free. Bound obtained by 3-signal photon per-year. ($g' = 1$)
- For DUNE detector, the sensitivity reach with active LAr of 40 kilotons, which corresponds to 1.085×10^{34} electrons inside the detector.
- The JUNO experiment will be equipped with liquid scintillator detector with fiducial mass of 20 kilotons, total number of electrons is 6.314×10^{33}.

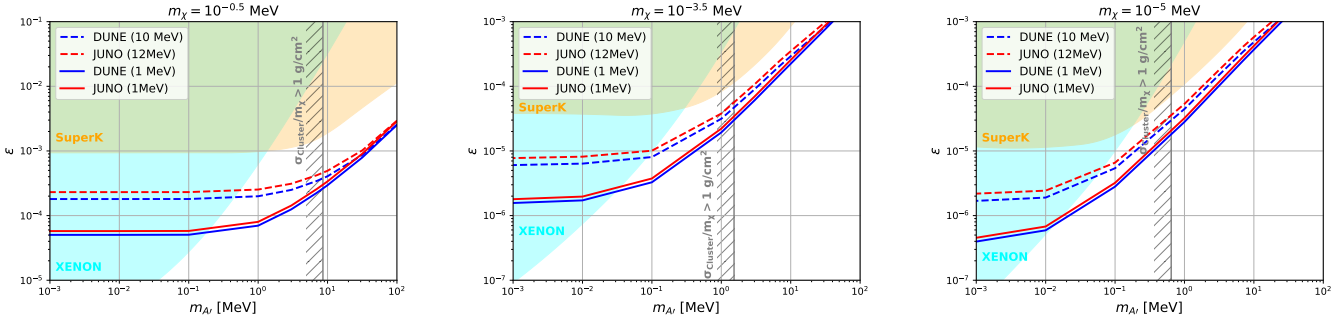

Conclusion

- CRDM offers a sensitive probe for light DM. Here, collinear splitting effects must be accounted for.
- In CRDM acceleration, the FSR effects suppress the boosted DM flux within the high-energy (high T_χ) region. The $A' \to \chi\chi$ production can enhance constraints from the PandaX-4T experiment in a narrow range.
- In CRDM detection, the PDF effects always reduce the experimental sensitivity. The collinear splitting induces dark Compton scattering; the mono-photon signal can possibly be probed at DUNE and JUNO.


Thank you!
四川大学物理学院